

Mathematical modelling of respiratory viral infection and applications to SARS-CoV-2 progression

Latifa Ait Mahiout¹, Nikolai Bessonov², Bogdan Kazmierczak³, and Vitaly Volpert⁴

¹Ecole Normale Superieure Kouba Sciences de l'Education

²Institut Problem Masinovedenia RAN

³Institute of Fundamental Technological Research Polish Academy of Sciences

⁴University of Lyon

June 25, 2022

Abstract

Viral infection in cell culture and tissue is modeled with delay reaction-diffusion equations. It is shown that progression of viral infection can be characterized by the viral replication number, time-dependent viral load and the speed of infection spreading. These three characteristics are determined through the original model parameters including the rates of cell infection and of virus production in the infected cells. The clinical manifestations of viral infection, depending on tissue damage, correlate with the speed of infection spreading, while the infectivity of a respiratory infection depends on the viral load in the upper respiratory tract. Parameter determination from the experiments on Delta and Omicron variants allows the estimation of the infection spreading speed and viral load. Different variants of the SARS-CoV-2 infection are compared confirming that Omicron is more infectious and has less severe symptoms than Delta variant. Within the same variant, spreading speed (symptoms) correlates with viral load allowing prognosis of disease progression.

Mathematical modelling of respiratory viral infection and applications to SARS-CoV-2 progression

L. Ait Mahiout^{1*}, N. Bessonov², B. Kazmierczak³, V. Volpert^{4,5,6†}

Laboratoire d'équations aux dérivées partielles non linéaires et histoire des mathématiques,
Ecole Normale Supérieure, B.P. 92, Vieux Kouba, 16050 Algiers, Algeria
Institute of Problems of Mechanical Engineering, Russian Academy of Sciences,
Saint Petersburg, Russia

Institute of Fundamental Technological Research, Polish Academy of Sciences, Warsaw, Poland
Institut Camille Jordan, UMR 5208 CNRS, University Lyon 1, 69622 Villeurbanne, France
INRIA Team Dracula, INRIA Lyon La Doua, 69603 Villeurbanne, France
Peoples Friendship University of Russia, 6 Miklukho-Maklaya St, Moscow, 117198, Russia

Abstract. Viral infection in cell culture and tissue is modeled with delay reaction-diffusion equations. It is shown that progression of viral infection can be characterized by the viral replication number, time-dependent viral load and the speed of infection spreading. These three characteristics are determined through the original model parameters including the rates of cell infection and of virus production in the infected cells. The clinical manifestations of viral infection, depending on tissue damage, correlate with the speed of infection spreading, while the infectivity of a respiratory infection depends on the viral load in the upper respiratory tract. Parameter determination from the experiments on Delta and Omicron variants allows the estimation of the infection spreading speed and viral load. Different variants of the SARS-CoV-2 infection are compared confirming that Omicron is more infectious and has less severe symptoms than Delta variant. Within the same variant, spreading speed (symptoms) correlates with viral load allowing prognosis of disease progression.

Keywords: viral infection, reaction-diffusion equations, viral load, spreading speed, SARS-CoV-2 variants

1 Introduction

SARS-CoV-2 infection spreads through the epithelial tissue from the upper respiratory tract (URT) to the bronchi and lungs (Ref. [2, 1]). Virus replicates in the infected cells that expel

*Alphabetic order of authors

†Corresponding author

viral particles into the extracellular space mainly through the apical surface (towards the airways) (Ref. [4, 3]), where they diffuse to the neighboring cells. As such, viral infection spreads in the tissue causing further clinical manifestations related to inflammation and tissue damage, while viral load produced in the URT determines infectivity of viral infection by means of virus-containing droplets. Thus, infection spreading speed and viral load represent important characterizations of viral infection. In this work, we use mathematical modelling in order to determine infection spreading speed and viral load, and we apply these results to characterize different variants of SARS-CoV-2 infection from the point of view of their infectivity and disease severity.

Bronchial epithelium is covered with the airway surface liquid (ASL) which consists of periciliary layer (PCL) and mucus produced by goblet cells. Coordinated motion of cilia at the surface of cilia cells moves ASL towards the pharynx (Ref. [5]). Mucus from the URT also moves to the pharynx but from the other side. Mucus protects the epithelial tissue from pathogens removing them with convective flow. It can also neutralize virus due to mucin molecules (Ref. [6]). SARS-CoV-2 can infect goblet and cilia cells and influence mucus production and motion (Ref. [7]). Moreover, mucus becomes more viscous in the infected tissue due to debris of viral particles and dead infected cells (Ref. [9]) and because more viscous mucus is produced due to infection and inflammation [8]. Furthermore, convective motion of ASL can influence infection spreading in the tissue. Thus, mucus motion should be taken into account in modelling respiratory infections.

Infection progression in cell cultures and tissues can be modelled with reaction-diffusion equations for the concentrations of uninfected cells, infected cells and virus (Ref. [10, 11]), while the innate and adaptive immune responses can be taken into account through the concentration of interferon, antigen presenting cells, and lymphocytes (in various ODE models, see, e.g., Ref. [12]). Analysis of these models shows that viral infection spreads in cell tissue as a reaction-diffusion wave (Ref. [13, 14, 11]). Such waves are mainly characterized by two parameters: the quantity of produced virus (viral load) and the speed of propagation. We determine them through the original model parameters, such as the rate of cell infection by virus and the virus replication rate in the infected cells, and we show that they are independent of each other in the sense that high (or low) viral load can be combined with high or low wave speed.

High viral load in the upper respiratory tract can be associated with a high rate of disease transmission (Ref. [15, 16]). However, low wave speed slows down disease progression in the lungs and, consequently, decreases disease severity. Recent animal studies show that, indeed, lung infection in the case of Omicron variant is low or not present at all (Ref. [17]). Moreover, cell culture and tissue experiments show that infection progression depends on cell types (Ref. [18, 19]). We use experimental data on time-dependent viral load from Ref. [18, 19] in order to identify model parameters and to characterize infection progression. In particular, we show that Omicron variant spreads faster in the upper respiratory tract than Delta variant and slower in the lungs, resulting in higher infectivity, shorter incubation period and less severe symptoms.

We model infection progression in the epithelial tissue taking into account mucus motion

in a two-phase reaction-diffusion model with a fluid flow in a two-dimensional strip and one-dimensional epithelial cell layer at the boundary of this strip (Section 2). We show that this model can be reduced to an one-dimensional two-phase model. This reduction allows us to find analytical expressions for the viral load and wave speed (Section 3). We apply these results to characterize Delta and Omicron variants in Section 4 and discuss the results in Section 5.

2 Infection progression in the epithelial tissue

Bronchial epithelium is covered with airway surface liquid (ASL) consisting of periciliary layer (PCL) and mucus and transported by the coordinate motion of cilia at the surface of cilia cells (Ref. [5]). In the process of viral infection, viral particles produced in the epithelial cells are expelled through the apical cell surface in the extracellular space where they diffuse and they are also transported by convective flow. Hence, studying infection progression in the epithelial tissue, we need to take into account ASL motion.

2.1 2D model

We consider a 2D problem in the domain $0 \leq x \leq L$, $0 \leq y \leq H$. Epithelial cell layer is considered as 1D interval located at the lower boundary $y = 0$, fluid is located in the whole rectangular domain, H is the width of the fluid layer (mucus and PCL). Approximation of constant layer width H implies that we do not consider mucus production and accumulation (Ref. [22]). This question will be considered in the forthcoming work.

Virus production in infected cells. We consider the system of equations

$$\frac{\partial U}{\partial t} = -aUV_c, \quad (2.1)$$

$$\frac{\partial I}{\partial t} = aUV_c - \beta I, \quad (2.2)$$

$$\frac{\partial V_c}{\partial t} = D_c \frac{\partial^2 V_c}{\partial x^2} + bI_\tau + pV_f - kV_c - \sigma_1 V_c \quad (2.3)$$

for the concentration U of uninfected cells, the concentration I of infected cells, the virus concentration V_c in the cell layer which includes epithelial cells and adjacent extracellular space. Next, $V_f(x, t) = V(x, 0, t)$ is virus concentration in fluid at the lower boundary, and $I_\tau(x) = I(x, t - \tau)$. Parameter a characterizes the rate of cell infection, b corresponds to the virus replication rate in the infected cells, β is the death rate of infected cells, σ_1 is the rate of virus death, parameters p and k characterize virus exchange between cell layer and fluid layer, D_c is virus diffusion coefficient in the cell layer. All these parameters are positive constants. A similar model without fluid was considered in the recent works [13, 14].

Virus distribution in fluid. Virus distribution in the fluid layer is described by the diffusion-convection equation

$$\frac{\partial V}{\partial t} = D_f \Delta V - u(y) \frac{\partial V}{\partial x} - \sigma_2 V, \quad (2.4)$$

where D_f is the diffusion coefficient, $u(y)$ is fluid velocity considered as a given function which can be approximated by a linear function in the PCL and constant in the mucus layer [22], σ_2 is the virus death rate in the fluid layer. This equation is completed by the boundary conditions:

$$x = 0, L : \frac{\partial V}{\partial x} = 0, \quad (2.5)$$

$$y = 0 : D_f \frac{\partial V}{\partial y} = h(pV(x, 0, t) - kV_c), \quad y = H : \frac{\partial V}{\partial y} = 0,$$

where h is the cell height, and initial condition $V(x, y, 0) = V_0$, $|x - x_0|^2 + |y - y_0|^2 \leq r^2$ which corresponds to a virus-containing droplet in the fluid layer.

Stationary distribution. We begin the study of problem (2.1)-(2.5) with the analysis of its stationary solutions in the cross-section of the layer (independent of x). It has a trivial stationary solution $V_c = V = 0$, $I = 0$. Neglecting death of infected cells ($\beta = 0$), we can find another stationary solution, independent of the space variable x and satisfying the equations

$$\frac{dI}{dt} = a(U_0 - I)V_c, \quad (2.6)$$

$$\frac{dV_c}{dt} = bI_\tau + pV_f - kV_c - \sigma_1 V_c \quad (2.7)$$

$$\frac{\partial V}{\partial t} = D_f \frac{\partial^2 V}{\partial y^2} - \sigma_2 V, \quad (2.8)$$

where $V_f(t) = V(0, t)$, and the boundary conditions:

$$y = 0 : D_f \frac{\partial V}{\partial y} = h(pV(x, 0, t) - kV_c), \quad y = H : \frac{\partial V}{\partial y} = 0. \quad (2.9)$$

We note that equations (2.1), (2.2) for $\beta = 0$ give the balance equation $I + U = U_0$, where U_0 is the initial concentration of uninfected cells. This balance equation allows us to reduce these two equations to equation (2.6). Searching stationary solution of this problem, we find $I = U_0$ from equation (2.6) and $V_c^s = (bU_0 + pV_f)/(k + \sigma_1)$. Then we obtain a closed problem for the stationary solution $V(y)$ (we keep for convenience the same notation):

$$D_f V'' - \sigma_2 V = 0, \quad (2.10)$$

$$D_f V'(0) = hpV(0) - \frac{kh(bU_0 + pV(0))}{k + \sigma_1}, \quad V'(H) = 0. \quad (2.11)$$

The solution of this problem is given by the following expression:

$$V^s(y) = \frac{K_2}{K_1(1 + e^{-2\mu H}) + \mu(1 - e^{-2\mu H})} (e^{\mu y - 2\mu H} + e^{-\mu y}), \quad (2.12)$$

where

$$\mu^2 = \frac{\sigma_2}{D}, \quad K_1 = hp \left(1 - \frac{k}{k + \sigma_1}\right), \quad K_2 = -\frac{khu_0}{k + \sigma_1}.$$

Let us note that for the considered range of parameters (e.g., Figure 1), the variation of the function $V(y)$ in the interval $0 \leq y \leq H$ is very weak (at most 0.1 %). This property of solution will allow us to reduce the 2D problem to a 1D problem.

Wave propagation. Viral infection propagates in the epithelial tissue as a reaction-diffusion wave if the influence of the boundary is negligible. From the mathematical point of view, it is a solution of problem (2.1)-(2.5) of the form $U(x, t) = \widehat{U}(x - ct)$, $I(x, t) = \widehat{U}(x - ct)$, $V_c(x, t) = \widehat{V}_c(x - ct)$, $V(x, y, t) = \widehat{V}(x - ct, y)$ considered for all real x with the limits

$$\begin{aligned} x = -\infty : U = 0, I = U_0, V_c = V_c^s, V = V^s(y), \\ x = \infty : U = U_0, I = V_c = V = 0 \end{aligned}$$

for $\beta = 0$, and $U(-\infty) = U_f, U(\infty) = U_0, I = V_c = V = 0$ at $x = \pm\infty$ for $\beta > 0$. The values V_c^s and $V^s(y)$ are determined in the previous section.

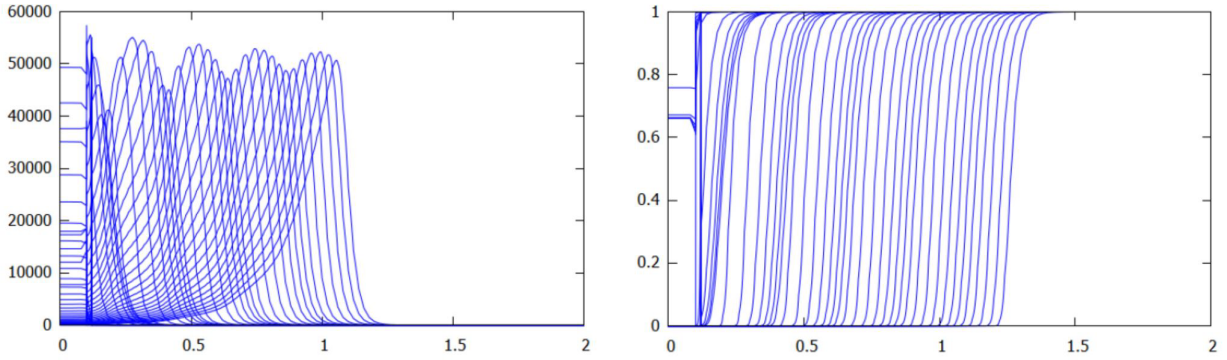


Figure 1: Virus distribution $V_c(x, t)$ in infected cell (left) and the concentration $U(x, t)$ of uninfected cells (right) in consecutive moments of time (every 1 hour). The values of parameters are as follows: $a = 0.1$ ($1/(\text{hour} \cdot \text{virus})$), $b = 8 \cdot 10^4$ ($\text{virus}/(\text{cell} \cdot \text{hour})$), $p = k = 0.1$ ($1/\text{hour}$), $D = 0.001$ (cm^2/hour), $D_c = 10^{-7}$ (cm^2/hour), $\beta = 0.1$ ($1/\text{hour}$), $h = H = 0.001$ (cm), $u(y) = 0$ (cm/hour), $\sigma_1 = \sigma_2 = 1$ ($1/\text{hour}$), $\tau = 10$ (hour).

Propagation of viral infection in the epithelial layer described by model (2.1)-(2.5) is shown in Figure 1 for the values of parameters determined in Ref. [13] for the SARS virus in the culture of cilia cells ((Ref. [3]). It is a typical reaction-diffusion wave of infection

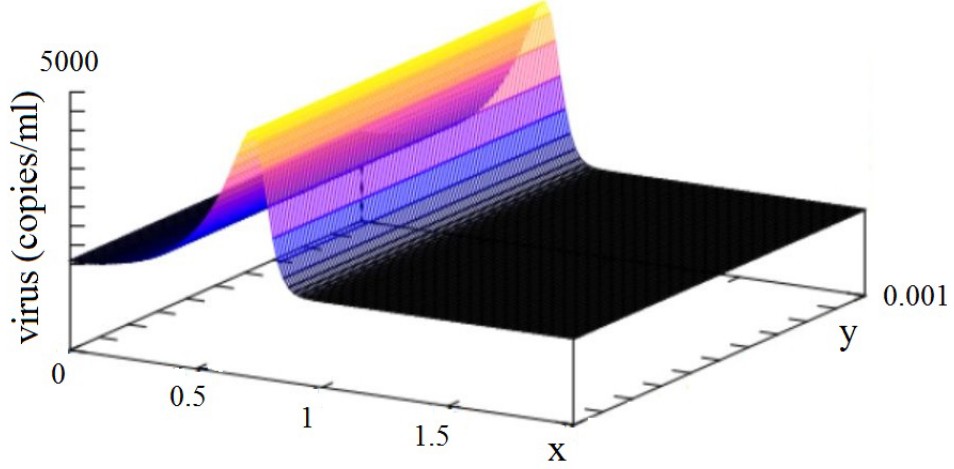


Figure 2: A snapshot of virus distribution in fluid for the same values of parameters as in Figure 1.

spreading. Damped oscillations are caused by the time delay in virus replication in the infected cells. Two-dimensional virus distribution in the fluid layer is shown in Figure 2. Its dependence on y is weak (less than 1%) since the fluid layer is narrow. This allows us to reduce the 2D problem to a one-dimensional two-layer problem.

2.2 Reduction to 1D model

Set $V_H = \frac{1}{H} \int_0^H V(x, y, t) dy$ and integrate equation (2.4) with respect to y . Then we obtain

$$\frac{\partial V_H}{\partial t} = D_f \frac{\partial^2 V_H}{\partial x^2} - \frac{h}{H} (pV(x, 0, t) - kV_c) - \frac{1}{H} \int_0^H u(y) \frac{\partial V}{\partial x} dy - \sigma_2 V_H. \quad (2.13)$$

Since the dependence of $V(x, y, t)$ on y is weak, that is, we can use the approximation $V(x, y, t) \approx V_f(x, t)$, then the last equation can be written as follows:

$$\frac{\partial V_H}{\partial t} = D_f \frac{\partial^2 V_H}{\partial x^2} - s \frac{\partial V_H}{\partial x} - \frac{h}{H} (pV_H - kV_c) - \sigma_2 V_H, \quad (2.14)$$

where

$$s = \frac{1}{H} \int_0^H u(y) dy$$

is an average flow velocity. Hence, we obtain the following 1D model:

$$\frac{\partial U}{\partial t} = -aUV_c, \quad (2.15)$$

$$\frac{\partial I}{\partial t} = aUV_c - \beta I, \quad (2.16)$$

$$\frac{\partial V_c}{\partial t} = D_c \frac{\partial^2 V_c}{\partial x^2} + bI_\tau + pV_H - kV_c - \sigma_1 V_c, \quad (2.17)$$

$$\frac{\partial V_H}{\partial t} = D_f \frac{\partial^2 V_H}{\partial x^2} - s \frac{\partial V_H}{\partial x} + \frac{h}{H}(kV_c - pV_H) - \sigma_2 V_H, \quad (2.18)$$

where V_c is virus concentration in cells, V_H its concentration in fluid, s is an average fluid velocity.

3 One-dimensional two-layer model

3.1 Virus reproduction number and viral load

Experimental data and mathematical modelling show that infection spreads in cell culture as a reaction-diffusion wave (Ref. [13]). In order to study this type of solutions, we consider system of equations (2.15)-(2.18) on the whole axis, and set $U(x, t) = u(x - ct)$, $I(x, t) = w(x - ct)$, $V_c(x, t) = v_1(x - ct)$, $V_H(x, t) = v_2(x - ct)$, where c is the wave speed. Then we obtain the following system of equations:

$$-cu' = -awv_1, \quad (3.1)$$

$$-cw' = awv_1 - \beta w, \quad (3.2)$$

$$-cv'_1 = bw + (pv_2 - kv_1) - \sigma_1 v_1, \quad (3.3)$$

$$-cv'_2 = v_2'' - sv_2' + \alpha(kv_1 - pv_2) - \sigma_2 v_2, \quad (3.4)$$

where prime denotes the derivative with respect to the variable $\xi = x - ct$, $\alpha = h/H$. We are interested in solution of this system of equations with the following limits at infinity:

$$u(-\infty) = u_f, \quad u(\infty) = u_0, \quad w(\pm\infty) = v_1(\pm\infty) = v_2(\pm\infty) = 0. \quad (3.5)$$

In this section we will determine u_f and viral load setting $\alpha = 1$ for brevity. From equation (3.1), we obtain

$$c \ln \frac{u_0}{u_f} = a \int_{-\infty}^{\infty} v_1(\xi) d\xi. \quad (3.6)$$

Taking a sum of (3.1), (3.2) and integrating:

$$c(u_0 - u_f) = \beta \int_{-\infty}^{\infty} w(\xi) d\xi. \quad (3.7)$$

Next, from (3.3):

$$\begin{aligned} b \int_{-\infty}^{\infty} w(\xi) d\xi + p \int_{-\infty}^{\infty} v_2(\xi) d\xi - k \int_{-\infty}^{\infty} v_1(\xi) d\xi \\ - \sigma_1 \int_{-\infty}^{\infty} v_1(\xi) d\xi = 0, \end{aligned} \quad (3.8)$$

and from (3.4):

$$k \int_{-\infty}^{\infty} v_1(\xi) d\xi - p \int_{-\infty}^{\infty} v_2(\xi) d\xi - \sigma_2 \int_{-\infty}^{\infty} v_2(\xi) d\xi = 0. \quad (3.9)$$

We denote the corresponding integrals by $I(v_1)$, $I(v_2)$, $I(w)$ and obtain from (3.8), (3.9):

$$I(v_1) = \frac{p + \sigma_2}{k} I(v_2), \quad I(w) = \left(\frac{(k + \sigma_1)(p + \sigma_2)}{k} - p \right) I(v_2).$$

We substitute these expressions into (3.6), (3.7) and finally obtain the equation

$$R_v(\omega - 1) = \ln \omega, \quad (3.10)$$

with respect to $\omega = u_f/u_0$. Here

$$R_v = \frac{abu_0(p + \sigma_2)}{\beta((k + \sigma_1)(p + \sigma_2) - kp)} \quad (3.11)$$

is the virus replication number. Equation (3.10) has a solution ω in the interval $0 < \omega < 1$ if and only if $R_v > 1$. The total viral load satisfies the equality

$$V_X^{(1)} \equiv \int_{-\infty}^{\infty} v_1(\xi) d\xi = -\frac{c}{a} \ln \omega, \quad (3.12)$$

where c is the wave speed. We can now determine $V_X^{(2)} \equiv \int_{-\infty}^{\infty} v_2(\xi) d\xi = kV_X^{(1)}/(p + \sigma_2)$.

Viral infections are usually characterized by large values of R_v . In this case, solution ω of equation (3.10) is close to 0, and $\ln \omega \approx -R_v$. Therefore, expression (3.12) for the total viral load can be written in the following form:

$$V_X^{(1)} = c \frac{bu_0(p + \sigma_2)}{\beta((k + \sigma_1)(p + \sigma_2) - kp)}, \quad (3.13)$$

$$V_X^{(2)} = c \frac{bku_0}{\beta((k + \sigma_1)(p + \sigma_2) - kp)}.$$

We will see in the next section that the wave speed c depends on a and b , while the remaining factor in (3.13) depends only on b (for other parameters fixed). Therefore, the wave speed and the total viral load can vary independently of each other, and they represent two different characterizations of viral infection.

3.2 Wave speed

Analytical formula for a simplified model. In order to obtain an analytical formula for the wave speed, consider a simplified model

$$\frac{\partial U}{\partial t} = -aUV, \quad (3.14)$$

$$\frac{\partial I}{\partial t} = aUV - \beta I, \quad (3.15)$$

$$\frac{\partial V}{\partial t} = D \frac{\partial^2 V}{\partial x^2} - s \frac{\partial V}{\partial x} + bI_\tau - \sigma V, \quad (3.16)$$

which does not take into account the difference in virus concentrations in the layer of epithelial cells and in the adjacent fluid layer. Using the linearization method (Ref. [13, 14]), we consider travelling wave solution $U(x, t) = \widehat{U}(x - ct)$, $I(x, t) = \widehat{I}(x - ct)$, $V(x, t) = \widehat{V}(x - ct)$ and we replace U by its value u_0 at ∞ . Therefore, we obtain the following system of equations for $\widehat{I}(x - ct)$, $\widehat{V}(x - ct)$:

$$cI' + au_0V + \beta I = 0, \quad (3.17)$$

$$Dv'' + (c - s)V' + bI(x + c\tau) - \sigma V = 0 \quad (3.18)$$

where we keep notation x for the independent variable and omit $\widehat{\cdot}$ for simplicity of notation. We look for a solution of this system in the form $I(x) = p_1 e^{-\lambda x}$, $V(x) = p_2 e^{-\lambda x}$. Substituting them in (3.17), (3.18), we obtain

$$-c\lambda p_1 + au_0 p_2 - \beta p_1 = 0,$$

$$D\lambda^2 p_2 - \lambda(c - s)p_2 + be^{-\lambda c\tau} p_1 - \sigma p_2 = 0.$$

We should find the minimal value of c for which this system of equation has a positive solution λ . Introducing an independent parameter $\mu = \lambda c$ and excluding p_1 and p_2 , we obtain the following equation:

$$D \frac{\mu^2}{c^2} + s \frac{\mu}{c} - \mu + \frac{abu_0}{\mu + \beta} e^{-\mu\tau} - \sigma = 0.$$

Hence,

$$c = \min_{\mu > \mu_0} F(\mu) \equiv \frac{2D\mu}{-s + \sqrt{s^2 + 4D(\mu + \sigma - abu_0 e^{-\mu\tau} / (\mu + \beta))}}, \quad (3.19)$$

where μ_0 is a positive solution of the equation $(\mu + \sigma)(\mu + \beta) = abu_0 e^{-\mu\tau}$. It is proved in Ref. [13] that for $s = 0$ this formula gives the exact value of the minimal wave speed. In general, it gives an estimate of the minimal wave speed from below. Numerical simulations confirm that we obtain the exact value of the minimal speed also for $s \neq 0$. This formula allows us to assess the dependence of the wave speed on parameters and to obtain an approximation of the wave speed for the two-layer problem.

Approximation of the wave speed for the two-layer problem. Comparison with numerical simulations show that the linearization method applied to the two-layer problem (2.15)-(2.18) gives an estimate from below for the minimal speed and not the exact value. Moreover, this estimate can be essentially different from the minimal speed, and it cannot be used as a reliable approximation. In order to obtain a better approximation of the minimal speed in this case, consider system (2.15)-(2.18) assuming for simplicity that $D_c = D_f$, $\sigma_1 =$

$\sigma_2, s = 0$. Set $V = V_c + V_H$. Suppose that $V_c = \kappa V$. Then we obtain the following system of equations:

$$\frac{\partial U}{\partial t} = -a\kappa UV, \quad (3.20)$$

$$\frac{\partial I}{\partial t} = a\kappa UV - \beta I, \quad (3.21)$$

$$\frac{\partial V}{\partial t} = D_\kappa \frac{\partial^2 V}{\partial x^2} - s(1 - \kappa) \frac{\partial V}{\partial x} + bI_\tau - \sigma V, \quad (3.22)$$

where $D_\kappa = \kappa D_c + (1 - \kappa) D_f$. We approximate κ by a constant and determine it from the limiting values of V_c and V_H at $-\infty$ (for $\beta = 0, p = k, H = h, \sigma_1 = \sigma_2 = \sigma$):

$$V_c = \frac{bu_0(k + \sigma)}{(k + \sigma)^2 - k^2}, \quad V_H = \frac{bu_0k}{(k + \sigma)^2 - k^2},$$

$\kappa = (k + \sigma)/(2k + \sigma)$. We can now apply formula (3.19) to this system. It gives a good approximation for 1D and 2D numerical results (Figure 3, left).

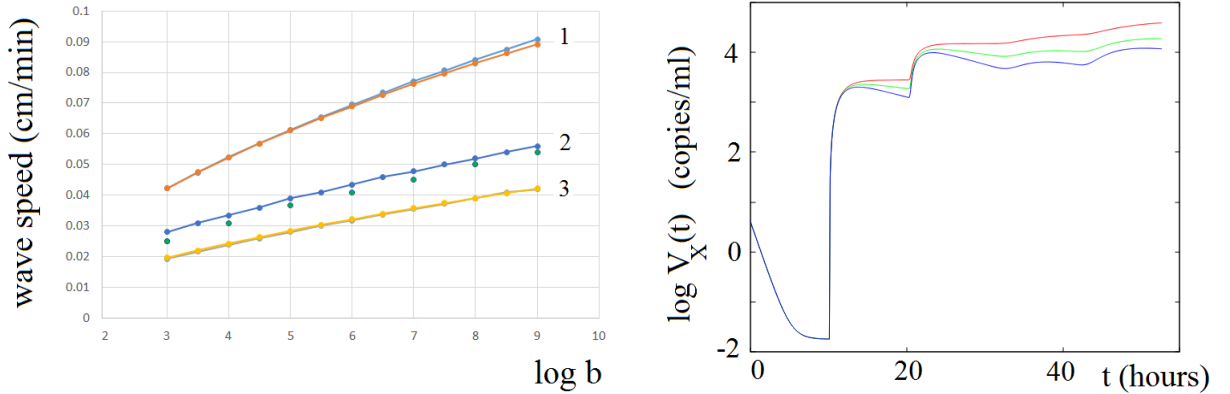


Figure 3: Left: wave speed in numerical simulations of system (2.15)-(2.18) (curves 1,2,3), in the analytical approximation with formula (3.19) (curves 1,3), and in 2D simulations (dots). In 1D case numerical results coincide with the analytical approximation given by formula (3.19), thus the corresponding approximating curves almost overlap. The values of parameters are as follows: $a = 0.1$ ($1/(\text{hour} \cdot \text{virus})$), $p = k = 0.1$ ($1/\text{hour}$), $D = 0.001$ (cm^2/hour), $\beta = 0$ ($1/(\text{hour} \cdot \text{cell})$) ($1/\text{hour}$), $h = H = 0.001$ (cm), $s = 0$; 1. $D_c = 0.001$ (cm^2/hour), $\sigma_1 = \sigma_2 = 1$ ($1/\text{hour}$), $\tau = 2$ (hour); 2. $D_c = 10^{-7}$, $\sigma_1 = \sigma_2 = 0.1$, $\tau = 5$; 3. $D_c = 0.001$, $\sigma_1 = \sigma_2 = 1$, $\tau = 8$. Right: viral load in in system (3.14)-(3.16) as a function of time. The values of parameters: $a = 0.01$, $b = 8 \times 10^5$, $\sigma = 1$, $s = 0$, $\kappa = 1$, $D_c = 0.001$, $\beta = 0$ (upper curve), $\beta = 0.05$ (middle curve), $\beta = 0.1$ (lower curve).

Dependence of the wave speed on parameters. From the analytical and numerical results we can make the following conclusions about the dependence of the wave speed on parameters.

- *Dependence on a and b .* Formula (3.19) shows that the wave speed depends on the product abu_0 and not on the individual parameters otherwise. Numerical simulations for system (2.15)-(2.18) confirm this conclusion for the whole range of parameters. Changing a and b up to the three order of magnitude in such a way that their product remains the same, the wave speed changes in the limit of 2 %. Dependence of the wave speed on b is shown in Figure 3. This dependence is weak, the wave speed changes at most 1.5 times when b changes by four orders of magnitude.
- *Dependence on D_c .* New viral particles produced by infected cells are expelled into extracellular matrix through their apical surface adjacent to the fluid layer (Ref. [3]). We will consider two different cases: either viruses diffuse only in the fluid ($D_c = 0$) or they also diffuse along the cell surface ($D_c \neq 0$). The difference between these two cases is not essential in the absence of fluid flow ($s = 0$) but it becomes essential for physiological values of fluid velocity (see below).
- *Dependence on s .* If virus diffusion occurs only in the fluid, then the wave speed dependence on the flow velocity is essential. For the flow velocity 10 cm/hour (lower estimate of physiological values), the wave speed against the flow becomes less than 10^{-3} cm/hour (for $b = 10^6$ and other parameters as in Figure 3). This means that viral infection will not arrive to the lungs from the URT during given time interval (in average 9 days according to the clinical data). Therefore, we need to assume non-zero diffusion in the cell layer. Furthermore, it should be of the same order of magnitude 0.001 cm²/hour as we take for fluid, otherwise the wave speed remains too small. If $D_c = D_f$, the wave speed against the flow does not depend on the flow velocity.
- *Dependence on other parameters.* Dependence of the wave speed on the replication delay τ is quite essential (Figure 3). Its dependence on β, k, p, σ_i is weak and not essential in the evaluation of infection progression.

Dependence of the viral load on parameters. The value of viral load during the third stage of infection progression (wave propagation) is given by the analytical formula (3.13). If we take the value c of the wave speed in numerical simulations, then we obtain exact correspondence between the analytical and numerical values of the viral load. An analytical approximation of the viral load during the previous two stages (decay to replication delay, explosive growth) can be constructed as a solution of delay differential equations (Ref. [14]). Dynamics of viral load in numerical simulations is shown in Figure 3 (right) for different values of the cell death coefficient β .

4 Characterization of Delta and Omicron variants

We compare the results of numerical simulations of infection progression in the epithelial tissue (without fluid motion) with the experimental data from Ref. [18, 19]. Experimental

results in human bronchial tissue show that viral load for Omicron is larger than for Delta during the first two days, but it becomes opposite at 72 hours. Parameters of the simulations are chosen to fit the data (Figure 4).

Since the values of parameters are important in order to characterize infection progression, let us briefly discuss how they are determined with the example of Figure 4 (left). The total viral load as a function of time has three consecutive stages: exponential decay before the beginning of virus replication, explosive growth in the beginning of replication, more slow growth during infection spreading. There are three steps of growth of viral load before it stabilizes at the maximal value (it can decrease or grow later depending on the value of β). The maximal viral load at 72 hours determines the value of b . The beginning of explosive growth depends on the value of τ , while the size of the first step (for a given value of b) depends on the value of a . Since the value of viral load V_{24}^O for Omicron at 24 h is not very different from the next two points, then V_{24}^O should be at the second step and, therefore, the time delay of replication τ_0 is less than 12 hours. It is different for Delta, since V_{24}^D should be at the first step and, therefore, τ_D is larger than 12 hours. The best results are obtained for $\tau_O = 10\text{h}$ and $\tau_D = 20\text{h}$. Let us note that these values can depend on the experimental conditions and they can be different from *in vivo* replication delays.

Let us note that the value of parameter a reflects the fact that only minor proportion of virus particles penetrate uninfected cells. This may be related to various cell protection mechanisms (Ref. [20, 21]) and to the experimental conditions (cf. Ref. [3]).

Analysis of the simulations allows us to conclude that Omicron starts to replicate faster than Delta in the bronchial tissue but slower in the lung tissue. The viral load is larger for Omicron during the first two days in the bronchial tissue, and smaller in the lung tissue (all three days). The speed of infection spreading in the bronchial tissue is $C_O = 0.012$ cm/hour and $C_D = 0.008$ cm/hour for Omicron and Delta, respectively. In the lung tissue, they are $C_O = 0.005$ cm/hour and $C_D = 0.008$ cm/hour. Thus, Delta variant preserves its spreading speed while it essentially decreases for Omicron.

It is interesting to note that the final value of the viral load for Delta in the bronchial tissue is larger than for Omicron, but its spreading speed is lower due to larger replication time. The viral load slowly decreases during further infection spreading due to death of infected cells. The virus replication number for both variants is the same in the bronchial tissue $R_v^D = R_v^O = 100$ but it is different in the lung tissue, $R_v^D = 300, R_v^O = 100$. We see that virus replication number is not sufficient to determine viral load and spreading speed. These three characteristics are independent of each other.

Comparison of viral load for Omicron and Delta variants in cell culture of human nasal epithelial cells and lung cells are presented in Ref. [19]. Parameter fitting and modelling of these results (not shown) confirm the conclusions about spreading speeds of the two variants in epithelial and lung tissues.

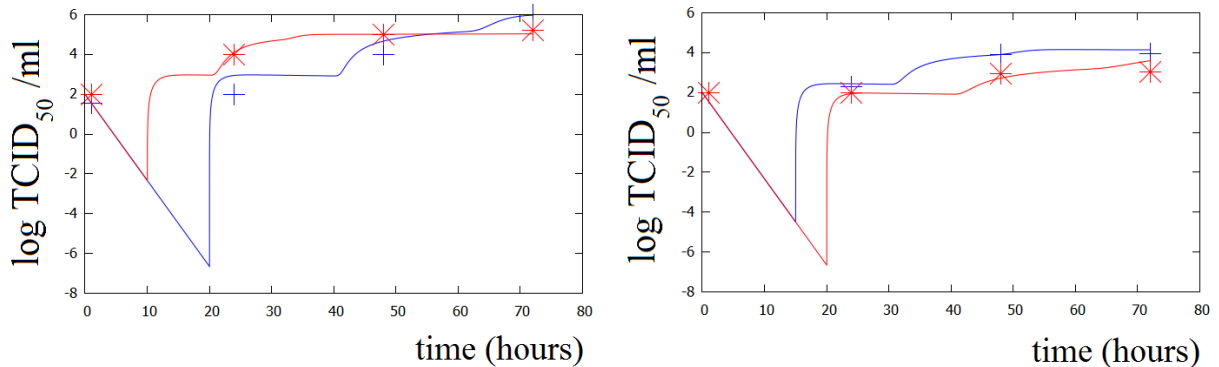


Figure 4: Total viral load as a function of time in the experiments in bronchial tissue and in numerical simulations for Delta (blue line, blue crosses) and Omicron (red line, red asterisks) variants. Left: bronchial tissue. The values of parameters for Delta: $a = 10^{-5}$, $b = 10^6$, $\beta = 0.01$, $\sigma = 1$, $\tau = 20$, $D = 0.001$, $L = 10$, $x_0 = 1$, $V_0 = 100$, $u_0 = 1$, for Omicron: $a = 10^{-4}$, $b = 10^5$, $\beta = 0.01$, $\sigma = 1$, $\tau = 10$, $D = 0.001$, $L = 10$, $x_0 = 1$, $V_0 = 100$, $u_0 = 1$. The initial condition is $V_0(x) = V_0$ for $0 \leq x \leq x_0$ and 0 otherwise. Experimental data are taken from Ref. [18]. Parameter dimensions are the same as in Figure 3. Tissue culture infectious dose (TCID₅₀) is a measure of virus titers. Right: lung tissue. The values of parameters for Delta: $a = 2 \cdot 10^{-4}$, $b = 1.5 \cdot 10^4$, $\tau = 15$, for Omicron: $a = 10^{-4}$, $b = 10^4$, $\tau = 20$ (other parameters are the same). Experimental data are taken from Ref. [18]. Parameter dimensions are the same as in Figure 3.

5 Discussion

Comparison of SARS-CoV-2 variants. Comparison of Delta and Omicron variants is carried out in this work on the basis of experimental data on viral load in cell cultures and tissues (Ref. [19, 18]). Different experimental conditions can influence the time-dependent viral load, and it can also differ from *in vivo* values. In particular, the replication delay in these experiments (10-20 hours) exceeds the estimates 6-7 hours in Ref. [2, 23]. Furthermore, the corresponding spreading speed is smaller than previously estimated for the SARS virus in Ref. [13] on the basis of the experiments in Ref. [3]. The latter is about 0.06 cm/hours (1.5 cm/day) in agreement with 9 day time interval for infection spreading from the URT to the lungs. Parameter estimates are consistent with other modelling studies (Ref. [24]).

However, different experimental results converge in relative comparison of viral loads for Delta and Omicron variants in the epithelial and lung tissue. Hence, based on different experiments we validate the conclusion that the spreading speed of Omicron variant is larger than the spreading speed of Delta variant in the epithelial tissue and smaller in the lung tissue.

Virus diffusion and convective transport. The estimates of infection spreading speed presented above allow us to evaluate the contribution of diffusive and convective transport.

An important conclusion from this analysis is that virus diffusion occurs in the cell layer (cells and adjacent extracellular space) where it is not influenced by convective transport. Furthermore, infection spreading speed from URT to the lungs (against fluid flow) does not essentially depend on the flow velocity due to diffusion in the cell layer. However, infection spreading in the opposite direction can be essentially accelerated by the flow.

Symptoms and infectivity. Clinical manifestation of viral infection related to tissue damage is not determined by the viral load itself but by the part of the infected tissue, that is, by the speed of infection spreading. As we discussed above, these are two different characteristics, though both of them are determined by the original model parameters. Hence, higher viral load can be associated with the same or even smaller wave speed. Indeed, since the wave speed depends on the product ab , we can vary these two parameters in such a way that their product remains constants. Then viral load is a linear function of b (see (3.13)), and for the same speed we can obtain any viral load. Thus, more severe or rapid symptoms can be observed for smaller viral load for different virus variants.

For a given variant, the parameters of the model are fixed, but inter-patient variation can be determined by the virus replication rate b which depends on the interferon concentration. Increasing b leads to the increase of the viral load (linearly proportional to b) and of the spreading speed ($\sim \sqrt{b}$). Hence, there is a correlation between the value of viral load in the URT and disease severity, in agreement with clinical observations (Ref. [26]). Thus, mathematical modelling can be used for the prognosis of disease progression.

Comparing the speeds of propagation for Delta and Omicron in different tissues, we can conclude that the incubation period for Omicron is about twice shorter than for Delta and its spreading in lungs is about twice slower.

Immune response. In the innate immune response, interferon produced by infected cells slows down virus replication rate. It is implicitly taken into account through the parameters of the model (cf. Ref. [13]) The influence of the adaptive immune response, which manifests itself on later stages of infection progression, will be considered in further works. We will restrict ourselves here by some remarks related to the previous analysis.

Denote by R_v^* the virus replication number taking into account the adaptive immune response. It is obtained from R_v replacing β by $\beta + \beta_c$, where β_c is the rate of infected cell elimination by cytotoxic lymphocytes CTL, and σ_i by $\sigma_i + \sigma_a$, where σ_a characterizes virus neutralization by antibodies. Adaptive immune response stops infection progression if $R_v^* < 1$. This condition, that is, the efficacy of the adaptive immune response in stopping infection is not directly determined by the viral load. Both of them can be expressed through the original model parameters, but they are not necessarily proportional to each other. Indeed, it follows from (3.13) that viral load is inversely proportional to β and can adopt high values for β small enough. Since $\beta \ll \beta_c$, then R_v^* depends on β_c and practically not β . Hence, the same result of the adaptive immune response can be obtained for very different viral loads.

Conclusions and perspectives. In this work we have determined the viral load and infection spreading speed for a generic respiratory viral infection and applied these results to characterize different variants of SARS-CoV-2 infection. More detailed description of mucus motion and of the immune response will be considered in the forthcoming works.

Acknowledgements

The third author was supported by the National Science Centre grant 2016/21/B/ST1/03071. The last author has been supported by the RUDN University Strategic Academic Leadership Program.

References

- [1] Vibhuti Kumar Shah et al. Overview of Immune Response During SARS-CoV-2 Infection: Lessons From the Past. *Front. Immunol.*, 07 August 2020 <https://doi.org/10.3389/fimmu.2020.01949>
- [2] J. P. Bridges, E. K. Vadar, H. Huang, R. J. Mason. Respiratory epithelial cell responses to SARS-CoV-2 in COVID-19. *Thorax* 2022;77:203209. doi:10.1136/thoraxjnl-2021-217561
- [3] A.C. Sims, R.S. Baric, B. Yount, S.E. Burkett, P.L. Collins, R.J. Pickles. Severe acute respiratory syndrome coronavirus infection of human ciliated airway epithelia: role of ciliated cells in viral spread in the conducting airways of the lungs. *Journal of Virology*, 79 (2005), no. 24, 15511-15524.
- [4] Y. Con, X. Ren. Coronavirus entry and release in polarized epithelial cells: a review. *Rev. Med. Virology*, 201, 24, 308-315.
- [5] W.L. Lee, P.G. Jayathilake, Zhijun Tan, D.V. Le, H.P. Lee, B.C. Khoo. Muco-ciliary transport: Effect of mucus viscosity, cilia beat frequency and cilia density. *Computers & Fluids*, 49 (2011), 214-221.
- [6] P. Gale. Thermodynamic equilibrium dose-response models for MERS-CoV infection reveal a potential protective role of human lung mucus but not for SARS-CoV-2. *Microbial Risk Analysis*, 16 (2020), 100140.
- [7] R. Robinot SARS-CoV-2 infection induces the dedifferentiation of multiciliated cells and impairs mucociliary clearance. *NATURE COMMUNICATIONS*, (2021) 12:4354 <https://doi.org/10.1038/s41467-021-24521-x>
- [8] D.K. Meyerholz, L.R. Reznikov. Influence of SARS-CoV-2 on airway mucus production: A review and proposed model. *Veterinary Pathology*, (2021), 1-8.

- [9] S. Girod, J-M. Zahm, C. Plotkowski, G. Beck, E. Puchelle. Role of the physicochemical properties of mucus in the protection of the respiratory epithelium. *Eur Resplr J* 1992, 5, 477-487.
- [10] Benjamin P. Holder, Philippe Simon, Laura E. Liao, Yacine Abed, Xavier Bouhy, Catherine A. A. Beauchemin, Guy Boivin. Assessing the in vitro fitness of an Oseltamivir-resistant seasonal A/H1N1 influenza strain using a mathematical model. *PLoS ONE*, 6 (2011), no. 3, e14767.
- [11] J. Yin, J. S. McCaskill Replication of viruses in a growing plaque: a reaction-diffusion model. *Biophys. Journal*, 61 (992), 1540-1549.
- [12] H. Y. Lee, et al. Simulation and Prediction of the Adaptive Immune Response to Influenza A Virus Infection. *Journal of Virology* Jun 2009, 83 (14) 7151-7165; DOI: 10.1128/JVI.00098-09
- [13] L. Ait Mahiout, N. Bessonov, B. Kazmierczak, G. Sadaka, V. Volpert. Infection spreading in cell culture as a reaction-diffusion wave. Submitted.
- [14] L. Ait Mahiout, B. Kazmierczak, G. V. Volpert. *Mathematics* 2022, 10, 256. <https://doi.org/10.3390/math10020256>
- [15] A. Marc et al. Quantifying the relationship between SARS-CoV-2 viral load and infectiousness. *eLife* 2021;10:e69302. DOI: <https://doi.org/10.7554/eLife.69302>
- [16] K. K. Bjorkman et al. Higher Viral Load Drives Infrequent Severe Acute Respiratory Syndrome Coronavirus 2 Transmission Between Asymptomatic Residence Hall Roommates. *The Journal of Infectious Diseases*, 2021:224, 1316-1324.
- [17] E. G. Bentley et al. SARS-CoV-2 Omicron-B.1.1.529 Variant leads to less severe disease than Pango B and Delta variants strains in a mouse model of severe COVID-19. *bioRxiv* preprint doi: <https://doi.org/10.1101/2021.12.26.474085>
- [18] M. C. W. Chan et al. SARS-CoV-2 Omicron variant replication in human respiratory tract ex vivo. *Biological Sciences*. DOI: <https://doi.org/10.21203/rs.3.rs-1189219/v1>
- [19] T. P. Peacock et al. The SARS-CoV-2 variant, Omicron, shows rapid replication in human primary nasal epithelial cultures and efficiently uses the endosomal route of entry. *bioRxiv* preprint doi: <https://doi.org/10.1101/2021.12.31.474653>
- [20] S. Majdoul, A. A. Compton. Lessons in self-defence: inhibition of virus entry by intrinsic immunity. *NATURE REVIEWs, Immunology*, 2021 <https://doi.org/10.1038/s41577-021-00626-8>
- [21] J. Yang, H. Yan. Mucosal epithelial cells: the initial sentinels and responders controlling and regulating immune responses to viral infections. *Cellular & Molecular Immunology* (2021) 18:16281630; <https://doi.org/10.1038/s41423-021-00650-7>

- [22] P Kurbatova, N Bessonov, V Volpert, H. A. W. M. Tiddens, C Cornu, P Nony, D Caudri. Model of mucociliary clearance in cystic fibrosis lungs. *Journal of Theoretical Biology* 372 (2015), 81-88.
- [23] J. Harcourt et al. Isolation and characterization of SARS-CoV-2 from the first US COVID-19 patient. bioRxiv preprint doi: <https://doi.org/10.1101/2020.03.02.972935>
- [24] J. S. Lord, M. B. Bonsall. The evolutionary dynamics of viruses: virion release strategies, time delays and fitness minima. *Virus Evolution*, 2021 doi: 10.1093/ve/veab039
- [25] G. Li, Y. Fan, Y. Lai, T. Han, Z. Li, P. Zhou, P. Pan, W. Wang, D. Hu, X. Liu, Q. Zhang, J. Wu. Coronavirus infections and immune responses. *J. Med. Virol.* 2020, 19.
- [26] J. Fajnzylber et al. SARS-CoV-2 viral load is associated with increased disease severity and mortality. *NATURE COMMUNICATIONS*, (2020) 11:5493 <https://doi.org/10.1038/s41467-020-19057-5>